LA-UR-97-556

CONF-970201--27

Title: Bulk Amorphous Metallic Alloys: Synthesis by Fluxing Techniques and Properties

Author(s): Yi He, CMS
Tongde Shen, CMS
Ricardo B. Schwarz, CMS

Submitted to: To be published in Metallurgical Transactions
1997 TMS Annual Meeting, February 9-13, Orlando, Florida

Los Alamos
NATIONAL LABORATORY

Form No. 836 R5
ST 2629 10/91

DISCLAIMER

BULK AMORPHOUS METALLIC ALLOYS:

SYNTHESIS BY FLUXING TECHNIQUES AND PROPERTIES

Yi He, Tongde Shen, and Ricardo B. Schwarz

Center for Materials Science, MS-K 765

Los Alamos National Laboratory

Los Alamos, NM 87545, U. S. A.

1997 TMS Annual Meeting, February 9-13, Orlando, Florida

1997 TMS Meeting, February 10-14, Orlando, Florida

BULK AMORPHOUS METALLIC ALLOYS:

SYNTHESIS BY FLUXING TECHNIQUES AND PROPERTIES

Yi He, Tongde Shen, and Ricardo B. Schwarz

Center for Materials Science, MS-K 765

Los Alamos National Laboratory

Los Alamos, NM 87545, U. S. A.

ABSTRACT

Bulk amorphous alloys having dimensions of at least 1 cm diameter have been prepared in the Pd-Ni-P, Pd-Cu-P, Pd-Cu-Ni-P, and Pd-Ni-Fe-P systems using a fluxing and water quenching technique. The compositions for bulk glass formation have been determined in these systems. For these bulk metallic glasses, the difference between the crystallization temperature T_x, and the glass transition temperature T_g, $\Delta T = T_x - T_g$, ranges from 60 to 110 K. These large values of ΔT open the possibility for the fabrication of amorphous near net-shape components using techniques such as injection molding. The thermal, elastic, and magnetic properties of these alloys have been studied, and we have found that bulk amorphous $Pd_{40}Ni_{22.5}Fe_{17.5}P_{20}$ has spin glass behavior for temperatures below 30 K.

I. INTRODUCTION

Undercooling phenomena in metallic melts are of significant importance because novel microstructures and phases can be explored by controlled undercooling and solidification.[1-7] In general, the microstructure developed on crystallizing the melt depends on the degree of undercooling at which crystallization takes place. Large degrees of undercooling are needed to obtain novel microstructures and amorphous alloys. Early studies on crystal nucleation by Turnbull and co-workers[8,9] demonstrated that the main competition to undercooling resided in oxides and other inclusions in the melt which acted as heterogeneous nucleation centers for crystallization. By using small droplets and emulsion techniques, they were able to isolate the heteronucleants and obtained relative undercoolings $\Delta T_{LN} / T_L$, where T_L is the liquidus temperature, on the order of 0.2 for a number of metallic elements. Other techniques, including containerless electromagnetic levitation[10-13] and fluxing,[5,14,15] have been used to extend the range of undercooling and study microstructure development from undercooled liquids, the magnetic properties of undercooled melts,[16] and the liquid-solid interfacial tension.[17] If heteronucleants are removed from the metallic melt, crystal nucleation will be homogeneous. The physics of homogeneous nucleation in undercooled metallic melts was developed by Turnbull and Fisher[18] following the earlier work of Gibbs and others.

Rapid solidification techniques can be used to extend the range of undercooling in metallic melts and produce amorphous alloys. To make an amorphous alloy, the metallic melt must be undercooled from the melting temperature T_L to the glass transition temperature T_g. Assuming that the melt has a low density of heteronucleants, the main competition to glass

formation will arise from homogeneous nucleation. Turnbull[19] studied homogeneous nucleation in undercooled melts and showed that the most important parameter describing the nucleation rate is the ratio $T_{rg} = T_g / T_L$ or reduced glass transition temperature. The solid curves in Figure 1 show homogeneous nucleation rates for various values of T_{rg} calculated using the parameters listed in ref. [20]. The nucleation rate becomes negligible for $T \rightarrow T_L$ (because the thermodynamic force for crystallization approaches zero) and for $T \rightarrow T_g$ (because the nucleation rate is kinetically suppressed by the increasing glass viscosity). If we associate a smaller nucleation rate (positive abscissa) with a larger time period during which the undercooled liquid can exist without crystallizing, the homogeneous nucleation rate curves in the figure become equivalent to the customary T-T-T or C-C-T curves for crystallization. It is then clear that during continuous cooling, the larger the value of T_{rg}, the smaller will be the critical cooling rate required to avoid crossing the nose of the C-C-T curve.

Because of the metallic bonding nature, the formation of metallic glasses usually requires high cooling rates, on the order of 10^6 K/sec, and amorphous metallic alloys cannot be produced in bulk forms. The recent discovery that a number of multicomponent alloys can be cooled from the melt to the amorphous state at cooling rates of only 1-100 K/sec has generated great interest.[21-27]

$Pd_{40}Ni_{40}P_{20}$ was one of the first bulk amorphous alloys discovered. Using water-quenching technique, Chen produced amorphous $Pd_{40}Ni_{40}P_{20}$ alloy rods with diameters of 1-3 mm.[28] Later, various techniques ranging from surface etching[29] and fluxing[30] were developed

to remove the heterogeneous nucleation centers in the molten $Pd_{40}Ni_{40}P_{20}$, enabling the production of cm-size glasses. All these studies addressed the particular composition of $Pd_{40}Ni_{40}P_{20}$. Recently, we reported the homogeneity range for bulk glass formation in the Pd-Ni-P system.[31,32] We found that bulk amorphous alloy rods with 10 mm in diameter can be produced over the composition range of 25-60 at.% of Pd and about 20 at.% of P. Using the fluxing technique, the bulk glass formation in the Pd-Cu-P system was discovered.[33]

In this study we use the fluxing technique to investigate the undercooling and vitrification in a number of glass-forming alloys: Pd-Ni-P, Pd-Cu-P, Pd-Cu-Ni-P, and Pd-Ni-Fe-P. All these bulk amorphous alloys have a wide temperature interval, $\Delta T = T_x - T_g$, between the glass transition temperature and the crystallization temperature. A large ΔT means that the undercooled liquid is stable against crystallization. It also has technological importance, because in this temperature range the undercooled liquid has low viscosity and thus can be processed into near-net shape components by techniques such as injection molding. Upon cooling the product, the glassy alloy recovers its room temperature strength which typically is on the order of 2 GPa. Figure 5 in [31] shows that when amorphous $Pd_{40}Ni_{40}P_{20}$ is heated to 340°C (within the ΔT range), a small pressure can be used to flow the glassy alloy into fine cavities.

II. EXPERIMENTAL

The bulk amorphous alloys were prepared by two synthesis methods. To prepare the Pd-Ni-P alloys, commercial Ni_2P powder (99.5% pure) was arc melted under a purified argon

atmosphere to produce Ni_2P ingots. Then, solid Ni_2P, palladium (99.99% pure), and nickel (99.99% pure) were arc-melted to form alloy ingots of the desired composition. These alloys were placed in fused silica tubes, and repeatedly purified in molten B_2O_3, as described in Refs. [29,30]. Finally, the fused silica tubes containing the melt and the flux were quenched in water.

To synthesize bulk amorphous Pd-Cu-P alloys, we started by ball-milling elemental powders of Pd (99.95% pure), Cu (99% pure), and P (99.99% pure) in a SPEX 8000 laboratory ball mill for about 10 hours. The ball-milling was carried out inside an argon-filled glove box containing less than 0.1 ppm oxygen. The ball-milled powder was then placed in a fused silica tube together with dehydrated B_2O_3 and processed as described above. The quenched Pd-Ni-P and Pd-Cu-P rods were sectioned with a low-speed diamond saw to prepare samples for x-ray diffraction, differential scanning calorimetry, and elastic moduli measurements.

The thermal stability and specific heat of the alloys were measured in a Perkin-Elmer differential scanning calorimeter, DSC-7. A sapphire single crystal was used as reference material for the specific heat measurements, as described before.[34]

For undercooling measurements, the prepared alloy ingot and dehydrated B_2O_3 were placed in fused silica tube. A chromel-alumel thermocouple sealed in a thin fused silica tube was immersed in the metallic melt. The silica tube containing the melt and the thermocouple was removed from the furnace and cooled in air. The temperature T_N at which undercooled liquid crystallized was registered by the thermocouple as a recalescence signal in the cooling curve.

III. BULK GLASS FORMATION

Bulk metallic glasses were obtained in the Pd-Ni-P, Pd-Cu-P, Pd-Cu-Ni-P, and Pd-Ni-Fe-P systems over wide ranges of composition.

A. *Pd-Ni-P System*

The solid symbols in Fig. 2 show the compositions at which we could prepare bulk amorphous rods with diameters of at least 10 mm. The glass forming range is restricted to a narrow band with phosphorus content close to 20 at.%. The palladium concentration can vary from 25 to 60 at.%. For most of these amorphous alloys, the difference $\Delta T = T_x - T_g$ is greater than 90 K.[31] Amorphous alloys are easiest to form at the $Pd_{40}Ni_{40}P_{20}$ composition, and cylinders 25-mm in diameter and 300 g in weight, can be easily produced.[31] Clearly, this size is not the upper limit for bulk glass formation in $Pd_{40}Ni_{40}P_{20}$.

B. *Pd-Cu-P System*

Figure 3 defines the compositions for the formation of 7-mm diameter bulk glasses in the Pd-Cu-P system. Similar to the Pd-Ni-P system, the glass formation range is restricted to near 20 at.% phosphorus. However, the palladium content for bulk glass formation is limited to 40-60 at.%, which is narrower than that for Pd-Ni-P alloys. Clearly, the glass forming ability for the Pd-Cu-P system is not as good as that of the Pd-Ni-P system.[33]

C. *Pd-Cu-Ni-P System*

Experience has shown that most bulk glass formers alloy have three or more components. Multicomponent alloys are thought to make crystallization more difficult (thus stabilize the melt) and the idea has been termed 'confusion principle'.[35] A quaternary alloy has an additional degree of freedom which may stabilize the melt and thus improve its glass forming ability. The results for Pd-Ni-P and Pd-Cu-P have shown that the glass forming range is restricted to about 20 at.% phosphorus. Thus, we only investigated quaternary alloys of the type $M_{80}P_{20}$ where M is a combination of Pd, Cu, Ni, and Fe.

Figure 4 shows the metal compositions for glass formation in the system $(Pd,Cu,Ni)_{80}P_{20}$. The minimum content of palladium needed for bulk glass formation (7-mm diameter rods) is about 25 at.%, similar to that in ternary Pd-Ni-P system. Amorphous 2-mm diameter balls were prepared at the composition $Pd_{20}Cu_{40}Ni_{20}P_{20}$.

D. *Pd-Ni-Fe-P System*

We found that 7-mm diameter amorphous rods could not be prepared in the ternary Pd-Fe-P system. Such rods can be prepared in the quaternary $(Pd,Ni,Fe)_{80}P_{20}$ system, as shown in Fig. 5. The metal range for bulk glass formation is considerably reduced from that in the $(Pd\text{-}Cu\text{-}Ni)_{80}P_{20}$ system.

IV. UNDERCOOLING OF BULK METALLIC MELTS

To understand what limits the glass formation in undercooled melts, it is important to measure the maximum degree of undercooling obtainable in the system. Figure 6 shows several continuous cooling curves for bulk $Ni_{40}Fe_{30}Pd_{10}P_{20}$ metallic melt fluxed in molten B_2O_3. The recalescence associated with crystallization is clearly seen in these curves. The lowest observed nucleation temperature in the undercooled melt was $T_N = 884$ K. Using differential thermal analysis (DTA), the equilibrium liquidus temperature of this alloy was determined to be $T_L = 1187$ K, and is shown by the horizontal line. The observed maximum undercooling for this alloy is thus $\Delta T = 303$ K, or about 0.26 T_L. From this figure, the average cooling rate between 1000 K and 900 K is estimated to be only about 5 K/sec. Certainly, the maximum undercooling will increase with increasing cooling rate. Table 1 lists the observed maximum undercooling for a number of alloys that did not form bulk glasses. It is interesting that the alloy $Ni_{40}Fe_{40}P_{20}$, which contains no palladium, can be undercooled to 0.27 T_L.

The use of undercooling curves, as those shown in Figure 6, to evaluate theories of homogeneous nucleation has always been a subject of controversy because no matter how clean the melt is, one can never be quite sure that the nucleation was not initiated at a weak heteronucleant. Thus, the present data represents a lower bound for the degree of undercooling that may be achieved in the presence of homogeneous nucleation alone. If we assume that the degree of undercooling is limited by homogeneous nucleation, then the lack of bulk glass formation in these alloys can be attributed to their relatively small T_{rg} values. For example, the

$Ni_{40}Fe_{30}Pd_{10}P_{20}$ alloy has $T_{rg} = 0.51$. We deduce this number form an estimated glass transition temperature of 600 K (see Table 2) and the measured liquidus temperature of 1187 K. Values of T_{rg} estimated for other alloys systems are included in Table 1.

V. THERMAL PROPERTIES

A. *Thermal Stability*

Figure 7 shows the DSC traces for four bulk glasses that are representative of the alloy systems studied. All alloys were measured at a heating rate of 20 K/min. Table 2 lists the values of T_g, T_x, T_L, T_{rg}, and the enthalpy of crystallization ΔH_x deduced from these curves. The temperature interval $\Delta T = T_x - T_g$ is a measure of the thermal stability of the undercooled liquid and all the bulk amorphous alloys studied here are characterized by large values of ΔT. For all the 10-mm diameter glassy Pd-Ni-P rods, ΔT was larger than 60 K, reaching 102 K at the composition $Pd_{40}Ni_{40}P_{20}$ (see Fig. 4 in Ref. [31]). For the glassy Pd-Cu-P alloys, ΔT ranges from 27 K to 73 K. For the quaternary glassy Pd-Cu-Ni-P alloys, ΔT ranges from 30 to 106 K, whereas for bulk glassy Pd-Ni-Fe-P, ΔT is about 60-70 K.

B. *Glass Transition Temperature*

The DSC results indicated that the glass transition temperature of $Pd_{80-x}Ni_xP_{20}$ is approximately constant, ranging from 576 to 588 K for x ranging from 20 to 55.[36] This weak composition dependence agrees with previously studies on rapidly solidified $Pd_{80-x}Ni_xP_{20}$

alloys,[37,38] where T_g was found to vary between 585 and 602 K, when x varies from 12 to 72. In contrast, T_g for bulk amorphous $Pd_{80-x}Cu_xP_{20}$ alloys decreases with increasing copper concentration x, as illustrated in Figure 8. The difference between the composition dependence of T_g in $Pd_{80-x}Ni_xP_{20}$ and $Pd_{80-x}Cu_xP_{20}$ may be due to the difference in the strength of the metal-metal interactions in these two alloys. The enthalpy of mixing of palladium and nickel in the liquid state is almost zero whereas that of palladium and copper is -14 kJ /(mole of atoms).[39] Chen[37] arrived to similar conclusions when comparing the composition dependence of T_g for glassy alloys of Pd-Ni-P, Pd-Co-P, and Pd-Fe-P prepared by rapid solidification.

The effect of copper on T_g appears also in the quaternary $(Pd\text{-}Ni)_{80-x}Cu_xP_{20}$ bulk amorphous alloys, as shown in Figure 9. The figure includes all the alloy compositions (black circles) in Figure 4. We notice then that the value of T_g depends on the copper content but not on the ratio of palladium and nickel in the alloy. The T_g data for $x > 10$ decreases linearly with increasing x. The figure also shows the liquidus temperature for some of these alloys measured by DSC. The T_L values also decrease linearly with increasing x. An exception to this behavior seems to be $Pd_{40}Cu_{30}Ni_{10}P_{20}$, which has an exceptionally low liquidus temperature. In agreement with this plot, all the quaternary bulk Pd-Ni-Cu-P alloys have roughly the same value of T_{rg}, ranging from 0.64 to 0.66. The exception is the alloy $Pd_{40}Cu_{30}Ni_{10}P_{20}$ which has $T_{rg} = 0.72$.

C. *Specific Heat*

Figure 10 shows the specific heat of $Pd_{40}Cu_{40}P_{20}$ measured at a heating rate of 10 K/min. The open circles are the C_p values of the as-prepared glass (associated with a cooling rate on the order of 100 K/s). The open triangles are the C_p values for the same glass after a pre-annealing treatment consisting of heating the sample in the DSC to 563 K and immediately cooling it to room temperature at a rate of about 1 K/s. The solid symbols give the specific heat of the crystallized alloy which was prepared by annealing the glassy sample at 673 K for 30 min. The large increase in C_p seen in the data of both glassy alloys near 550 K is caused by the glass transition, which is reversible. The difference between the data for the as-prepared and annealed glasses in the range 475 to 560 K is due to an irreversible structural relaxation in the as-prepared glass. This relaxation can be explained by the free volume model,[40-43] as discussed in detail by van den Beukel and Sietsma.[44] In essence, the as-prepared bulk amorphous alloy contains an excess free volume trapped in the structure which is not in equilibrium at the temperature of the measurements. When the alloy is heated to a temperature close to T_g, atom rearrangements becomes possible on a local scale and the excess free volume relaxes towards the equilibrium value. This process, often called topological short range ordering, releases internal energy and thus the apparent C_p is smaller.

Figure 11 shows similar C_p measurements for $Pd_{40}Ni_{40}P_{20}$ alloys. The solid circles gives the specific heat of the crystallized alloy prepared by annealing the amorphous sample at 823 K for 30 min. X-ray diffraction shows that crystallized $Pd_{40}Ni_{40}P_{20}$ contains an fcc (Pd-Ni)

solid solution which is magnetic. The small kink in the otherwise straight C_p data for the crystallized alloy is due to the magnetic transition of the nickel-rich fcc solid solution. This peak will be further discussed below. The C_p data for the *as-prepared* $Pd_{40}Ni_{40}P_{20}$ (open circles) alloy shows a small decrease in the temperature range $400 < T < 525$ K, quite similar to that seen in the $Pd_{40}Cu_{40}P_{20}$ data (Fig. 10), which we attribute to an irreversible densification. The C_p data for the annealed and slowly cooled amorphous $Pd_{40}Ni_{40}P_{20}$ alloy (open triangles), however, is quite different from that for the annealed and slowly cooled amorphous $Pd_{40}Cu_{40}P_{20}$ alloy. On heating the annealed $Pd_{40}Ni_{40}P_{20}$ alloy in the range $400 < T < 575$ K, the C_p data is higher than that of the as-prepared alloy by as much as 10%. This increase in C_p cannot be explained by a free volume reduction. The fact that the increase is present in the $Pd_{40}Ni_{40}P_{20}$ alloy and not in the $Pd_{40}Cu_{40}P_{20}$ alloy suggests that the effect is related to the chemical interaction of the metal atoms. We offer the following tentative explanation. While the amorphous $Pd_{40}Ni_{40}P_{20}$ is slowly cooled below its glass transition, atom rearrangements occur in response to a lowering of the stored elastic energy in the amorphous structure. This can easily occur in the $Pd_{40}Ni_{40}P_{20}$ alloy since nickel and palladium have a near-zero heat of mixing. Because Ni and Pd have largely different atomic sizes, the atomic rearrangements are driven by a release of atom-scale internal stresses. The release of internal stress is more difficult when slowly cooling amorphous $Pd_{40}Cu_{40}P_{20}$ alloy because Pd and Cu have a negative heat of mixing (-14 kJ/mole). The

rearrangement of the metal atoms could be local (near neighbor interchanges) or diffusional (e.g., spinodal decomposition). On re-heating the $Pd_{40}Ni_{40}P_{20}$ alloy to temperatures approaching T_g, the order introduced on slow cooling is destroyed on account of the entropy of mixing and this appears on the DSC trace as an endothermic event. Notice further that a small endothermic excess heat appears also in the DSC trace for the as-prepared $Pd_{40}Ni_{40}P_{20}$. Indeed, comparing the DSC curves for the as prepared $Pd_{40}Ni_{40}P_{20}$ and $Pd_{40}Cu_{40}P_{20}$ alloys one can visualize that in the absence of the chemical order, the DSC trace for the as-prepared $Pd_{40}Ni_{40}P_{20}$ alloy would have looked as indicated by the dashed line. Thus, the ordering seems to be fast and may even occur during the initial slow heating in the DSC.

Figure 12 shows similar specific heat data for as-prepared and annealed $Pd_{40}Ni_{20}Fe_{20}P_{20}$. The annealing was performed in DSC by heating the as-prepared sample to 633 K at 20 K/min, and held for 3 min before cooling to room temperature at 20 K/min. For both the as-prepared and annealed and then slowly cooled glasses, C_p shows an anomalous increase between 500 and 580 K which we attribute to a chemical disordering among the metal atoms. This endothermic signature has sometimes been identified as 'second' glass transition.[45,46] Our structural studies using synchrotron X-ray diffraction show evidence of a phase separation after annealing glassy $Pd_{40}Ni_{40}P_{20}$ at 523 K for 30 min.[47] More detailed studies are in progress.

The crystallized $Pd_{40}Ni_{40}P_{20}$ contains a magnetic phase. The Curie temperature of the magnetic transition can be determined from the specific heat measurements, as shown in Figure 11 (solid circles), and on an enlarged scale in Figure 13. X-ray diffraction showed that

crystallized $Pd_{40}Ni_{40}P_{20}$ contains an fcc (Pd-Ni) solid solution and other metal phosphide phases. Because the equilibrium solubility of P in either Pd or Ni is very small, we assume that the Pd-Ni solid solution contains no phosphorus. Using the measured Curie temperature of $T_C = 514$ K and the published Curie temperature of Pd-Ni solid solutions,[48] we deduce that the composition of the Pd-Ni phase in our alloys is close to $Ni_{60}Pd_{40}$. This result agrees with the work of Donovan *et al.*[49] who, using transmission electron microscopy (TEM) and X-ray microanalysis, identified the composition of this phase to be $Ni_{59}Pd_{40}P_1$. The other two crystalline phases in the alloys were reported as $Pd_{34}Ni_{45}P_{21}$ and $Pd_{68}Ni_{14}P_{18}$.

VI. CRITICAL COOLING RATE FOR GLASS FORMATION

Using the fluxing technique, Lau and Kui [50] determined that the critical cooling rate for forming a 7-mm diameter bulk amorphous $Pd_{40}Ni_{40}P_{20}$ cylinder was ~ 0.75 K/sec. From this value, they estimated that the maximum steady-state nucleation frequency was on the order of 10^4 m^{-3} s^{-1}. On the other hand, Drehman and Greer [51] estimated that the steady state nucleation frequency at 590 K is approximately 10^6 m^{-3} s^{-1}, which is also the maximum nucleation frequency. These two values are the smallest ever found in a metallic system. From the measured nucleation frequency and an estimated crystal growth rate of ~ 10^{-10} m/s at 590 K, follows that the *theoretical* critical cooling rate for glass formation in $Pd_{40}Ni_{40}P_{20}$ is 10^{-3} K/s.

There have been various attempts to measure the critical cooling rate in $Pd_{40}Ni_{40}P_{20}$. Willnecker *et al.* [52] reported an upper bound of 0.17 K/s. Using the fluxing technique, we found that mm-size $Pd_{40}Ni_{40}P_{20}$ liquid can be vitrified without crystallization at a cooling rate of 0.34 K/s.[53] For such a low critical cooling rates, the thermodynamic properties of the undercooled $Pd_{40}Ni_{40}P_{20}$ liquid can be measured for the first time over the entire undercooling regime, from the melting temperature down to the glass transition temperature.[54] In comparison, the critical cooling rate for glass formation in the multi-component $Zr_{41.2}Ti_{13.8}Cu_{12.5}Ni_{10}Be_{22.5}$ alloy is ~ 1 K/s.[55] Our work to date suggests that the critical cooling rates in the quaternary Pd-Cu-Ni-P alloys are even smaller than those reported for the ternary Pd-Ni-P alloys.

VII. ELASTIC PROPERTIES

Understanding the elastic properties of a material is essential for engineering applications. The present availability of bulk glassy alloys allows us to determine their elastic properties using a resonant ultrasound spectroscopy.[33,36] In this technique, the spectrum of the mechanical resonance of a parallelepiped sample is measured and compared with a theoretical spectrum calculated for a given set of elastic constants. The true set of elastic stiffness constants is calculated by a recursive regression method that optimizes a match between the two spectra. Further details of this technique have been described elsewhere.[56-58]

An isotropic amorphous alloy has only two independent second order elastic stiffness constants. The room-temperature elastic moduli for a number of bulk amorphous alloys are

listed in Table 3. Table 3 also lists the density ρ of these bulk glasses, which was measured using the Achemedes' method with pure ethanol as immersion fluid. The last column in the table lists the Debye temperature of the alloys, deduced from the measured room temperature elastic constants and density. For the same Pd and P content, Ni-containing glasses have slightly higher elastic moduli and Debye temperatures than the corresponding Cu-containing glasses. The general trend in the Debye temperature data agrees with the fact that the Debye temperature of the metallic elements decreases in the order of Ni to Cu to Pd.

VIII. MAGNETIC PROPERTIES OF Pd-Ni-Fe-P ALLOYS

Magnetic susceptibility measurements show that bulk glassy Pd-Ni-Fe-P alloys are spin glasses below approximately 30 K. Figure 14 shows the field-cooled and zero-field-cooled susceptibility for as-prepared bulk amorphous $Pd_{40}Ni_{22.5}Fe_{17.5}P_{20}$ alloy as a function of temperature. The susceptibility was measured at a DC field of 10 Gauss. The field cooled curves are reversible whereas the zero-field-cooled is not. At any constant temperature below 30 K, the susceptibility in the zero-field-cooled state drifts upwards with increasing temperature. This change is irreversible. Additional evidence for spin glass behavior comes from measurements of magnetic hysteresis, field dependence of the thermoremanent magnetization (TRM), isothermal remanent magnetization (IRM), and time relaxation of the TRM and IRM. These results will be presented elsewhere.

IX. DISCUSSION AND CONCLUSIONS

Our experimental results indicate that the removal of heterogeneous nucleation sites is essential for bulk glass formation. When melts of the type $(Pd\text{-}M)_{80}P_{20}$, where M is one or more of the elements Ni, Cu, and Fe, are fluxed in molten B_2O_3, heterogeneous nucleation centers can be chemically reduced and/or dissolved in the flux. Then, the major competition to glass formation comes from homogeneous crystallization. Using this fluxing technique, bulk amorphous alloys in the Pd-Ni-P, Pd-Cu-P, Pd-Cu-Ni-P, and Pd-Ni-Fe-P systems were produced at cooling rates on the order of 100 K/s.

Glass formation with less than 20 at.% Pd seems unlikely in the systems studied. Air undercooling experiments (cooling rate on the order of 5 K/s) were studied on a variety of alloys which did not form glasses upon quenching in water. Molten $Pd_{10}Ni_{40}Fe_{30}P_{20}$ can be undercooled by 303 K, or 0.26 T_L. Because most of these alloys have similar values of T_g, the difficulty in bulk glass formation is attributed to the high value of T_L which leads to a small value of T_{rg}.

The removal or neutralization of the heteronucleants is a necessary but not a sufficient condition for bulk glass formation. An additional requirement, as discussed by Turnbull,[19] is a small $T_L - T_g$ labile regime or alternatively, a large reduced glass transition temperature, T_g / T_L. This requires stabilizing the liquid with respect to the crystalline phases, which can be accomplished either by stabilizing the liquid, de-stabilizing the crystal, or by both effects acting simultaneously.

A large number of solutes helps stabilize the liquid with respect to an ordered compound through the entropy of mixing. The liquid can be further stabilized through topological short-range ordering (TSRO). The preferred TSRO in a metallic liquid is based on the packing of tetrahedra since this results in a more efficient volume filling. In single-component liquids, polytetrahedral packing is limited by frustration, the geometric inability to form large tetrahedral aggregates unless some of the interatomic bonds are severely stretched or compressed.[59] Clearly, geometrical frustration is easier to accommodate if the melt contains atoms of various sizes and the *chemical interaction between these atoms is weak.* In metal-metalloid glasses, the metalloid atoms avoid being nearest neighbors to each other, and the local atomic configurations is dominated by trigonal bi-prisms with the metalloids at their centers and metal atoms at the corners and faces.[60] If the glass contains more than one metallic species, and the metal atoms have near zero heats of mixing, the undercooled liquid will be able to relax the atomic-level stresses as its becomes a glass. If instead the metal atoms have large heats of mixing, either positive or negative, the metal atoms will not be free to choose their neighbors at will, and thus will not be able to effectively relax the atomic-level stresses in the glass.

The ability of atoms with near-zero heat of mixing to relax atomic-level stresses may explain the excellent glass forming ability in the $(Pd,Ni,Cu,Fe)_{80}P_{20}$ systems. Pd and P, and Ni and P, have both large negative heats of mixing, whereas Pd and Ni have a near zero heat of mixing in the liquid (amorphous) state. The present specific heat measurements (Figs. 11 and 12) show that at temperatures about 100 K below T_g, there is change in the chemical order in the glass which cannot be explained by the free volume model. We also noticed that this change is absent in the Pd-Cu-P system, and we attribute this to the slight negative heat of mixing between

Cu and Pd. We suggest that the ability of the metal atoms in the Pd-Ni-P glasses to relax atomic-level stresses is the reason why Pd-Ni-P is a better glass forming system than Pd-Cu-P.

Having atoms with near-zero heat of mixing may also explain the good glass forming ability of the $Zr_{41.2}Ti_{13.8}Cu_{12.5}Ni_{10}Be_{22.5}$ alloy and of similar atoms that do not contain beryllium. In fact, this alloy has two pairs of atoms, (Zr, Ti), and (Cu, Ni) which have near-zero heat of mixing. Another example supporting this idea in the bulk glass former $La_{55}Al_{25}Ni_{20}$. This ternary alloy can be cast into 3-mm diameter amorphous rods.[61] The partial replacement of the nickel by copper and cobalt increases significantly the glass forming ability of this alloy, enabling the production of 9-mm diameter amorphous $La_{55}Al_{25}Ni_{10}Cu_5Co_5$ rods.[23] In this alloy, nickel, copper and cobalt have all near zero or slightly positive heats of mixing.[39]

Polytetrahedral aggregates cannot by themselves form a crystal without introducing systematic distortions.[62] If the TSRO in the polytetrahedral liquid aggregates is different from the structural order in the crystals that the alloy can form, then the crystallization of the undercooled melt will require first a dissolution of the polytetrahedral TSRO, followed by the formation of the crystalline nuclei, which presumably includes octahedral groups. This reconstruction is more difficult when the melt has the 'wrong' TSRO.[63] A more efficient atomic packing in the undercooled melt should also affect the kinetics of crystallization by decreasing the atomic mobility, and thus slowing any solute partitioning that may be necessary for crystal nucleation and growth.

A large number of vastly different atomic sizes not only stabilizes the melt, but also de-stabilizes the crystal since it is less likely to find crystalline structures that can accommodate a

large variety of atomic sizes at arbitrary concentrations. Greer has termed this the *principle of confusion*,[35] following ideas set forth by Waseda and Egami.[64]

In conclusion, from a *macroscopic* viewpoint, the formation of bulk amorphous alloys via the solidification of melts requires firstly the removal or neutralization of all heteronucleants from the melt, and secondly, a large value of T_{rg}, most likely in excess of 0.6. The next question is, what are the *microscopic* requirements for a large T_{rg} value, or equivalently, low T_L and high T_g values? It has long been known that a low T_L (deep eutectic) can be obtained in binary alloys of atoms having a large negative heat of mixing and vastly different atomic sizes (atomic radii differing by more than 10%). Strong atomic interactions give the melt atomic directionality whereas a large atomic size difference reduces the number of crystalline compounds which can form in the undercooled melt. The present research suggests that the binary melt can be further stabilized by adding a third element which has an atomic size different to that of the other two components and, equally important, has a very low heat of mixing with one of the previous components. This additional degree of freedom gives the melt the means to relax atomic scale internal stresses, making it more stable. Certainly, this argument can be further extended to alloys with four and more components.

ACKNOWLEDGMENTS

The authors thank Dr. A. Migliori for facilitating his ultrasound spectroscopy apparatus for the elastic constants measurements. This work was supported by the U. S. Department of Energy, Office of Basic Energy Sciences, Division of Materials Sciences.

Figure Captions

Figure 1 Homogeneous nucleation rate as a function of reduced temperature, T_r, for three values of the reduced glass transition temperature, T_{rg}.

Figure 2 Bulk glass formation range in Pd-Ni-P system. Filled circles denote the formation of glassy rods with diameters of at least 10 mm. Open circles represent compositions at which the rods were crystalline.

Figure 3 Bulk glass formation range in the Pd-Cu-P system. Filled circles denote the formation of glassy rods with diameters of at least 7 mm.

Figure 4 Bulk glass formation range in the quaternary Pd-Cu-Ni-P system. The phosphorus concentration is kept at 20 at.%. Filled circles denote the formation of glassy rods with diameters of at least 7 mm. Open triangles indicate that the 7-mm rod is partially amorphous; open circles denote crystalline rods. Thick black lines indicate the bulk glass formation range in the ternary alloys $Pd_{80-x}Ni_xP_{20}$ and $Pd_{80-x}Cu_xP_{20}$.

Figure 5 Bulk glass formation range for $(Pd,Ni,Fe)_{80}P_{20}$. Filled circles indicate the formation of 7-mm diameter amorphous rods. The thick black line indicates the bulk glass formation range in the ternary $Pd_{80-x}Ni_xP_{20}$.

Figure 6 Continuous cooling curves for 5-gram $Ni_{40}Fe_{30}Pd_{10}P_{20}$ melts. The equilibrium liquidus temperature determined by DTA measurements is indicated by a horizontal line. T_N indicates the recalescence temperature.

Figure 7 DSC traces for bulk amorphous alloys representative of the alloy systems studied. The DSC scanning rate was 20 K/min. T_g and T_x are defined as the onsets of the glass transition and crystallization temperatures.

Figure 8 Composition dependence of the glass transition temperature in bulk amorphous $Pd_{80-x}Cu_xP_{20}$ alloys.

Figure 9 Composition dependence of the glass transition temperature (solid circles) and the liquidus temperature (open triangles) in glassy $(Pd,Ni)_{80-x}Cu_xP_{20}$ alloys.

Figure 10 Specific heat of as-prepared, annealed (to 563 K), and crystallized $Pd_{40}Cu_{40}P_{20}$ determined by DSC at the scanning rate of 10 K/min.

Figure 11 Specific heat of as-prepared, annealed, and crystallized glassy $Pd_{40}Ni_{40}P_{20}$ measured at a heating rate of 20 K/min.

Figure 12 Specific heat of as-prepared and annealed glassy $Pd_{40}Ni_{20}Fe_{20}P_{20}$ measured at a heating rate of 20 K/min.

Figure 13 Specific heat of crystalline $Pd_{40}Ni_{40}P_{20}$ showing the Curie temperature $T_c = 514$ K.

Figure 14 Susceptibility (χ) of as-prepared bulk amorphous $Pd_{40}Ni_{22.5}Fe_{17.5}P_{20}$ measured at a DC field of 10 Gauss. The sample was first cooled to about 5 K at zero field and χ was measured during warming (open circles). The χ measurements were repeated for field cooling (upper triangles) and field warming (down triangles).

Table 1

Maximum undercooling for a number of Fe-containing alloy melts cooled at about 5 K/s in B_2O_3 flux. T_L is the liquidus temperature, T_N is the lowest temperature at which crystal nucleation takes place, and $\Delta T_{LN} = T_L - T_N$ is the maximum undercooling. T_g is the glass transition temperature and T_{rg} is the reduced glass transition temperature.

Alloy	Sample weight	T_L (K)	T_N (K)	ΔT (K)	T_g	T_{rg}	$\Delta T/T_L$
$Ni_{40}Fe_{40}P_{20}$	4.9 g	1249	913	336	650[a]	0.52	0.27
$Ni_{40}Fe_{30}Pd_{10}P_{20}$	5.0 g	1187	884	303	600[b]	0.53	0.26
$Ni_{40}Fe_{20}Pd_{20}P_{20}$	5.3 g	1123	886	237	600[b]	0.53	0.21
$Fe_{80}P_{20}$	15.0 g	1383	1128	255	650[a]	0.47	0.18
$Fe_{82}B_{18}$	14.5 g	1448	1264	185	760[a]	0.52	0.13

a: data taken from table 1 in ref.[65]

b: estimated from the glass transition temperature of bulk Pd-Ni-Fe-P glasses (see Table 2).

Table 2

T_g, T_x, ΔT, T_L, T_{rg}, and ΔH_x for bulk amorphous Pd-Ni-P and Pd-Cu-P alloys determined by DSC at a scanning rate of 20 K/min. The samples were cut from 7-mm diameter rods unless indicated otherwise.

Composition	T_g (K)	T_x (K)	ΔT (K)	T_L (K)	T_{rg}	ΔH_x (kJ/mole)
$Pd_{30}Ni_{50}P_{20}$	583	673	90	1010	0.58	5.94
$Pd_{40}Ni_{40}P_{20}$	576	678	102	991	0.58	7.37
$Pd_{50}Ni_{28}P_{22}$	584	676	92	972	0.60	6.06
$Pd_{40}Cu_{40}P_{20}$	548	599	51	843	0.65	2.66
$Pd_{50}Cu_{30}P_{20}$	562	619	57	863	0.65	3.92
$Pd_{60}Cu_{20}P_{20}$	596	660	64	916	0.65	4.04
$Pd_{20}Cu_{40}Ni_{20}P_{20}$ (*)	551	608	57	807	0.68	1.55
$Pd_{25}Cu_{30}Ni_{25}P_{20}$	572	615	43	863	0.66	3.81
$Pd_{30}Cu_{30}Ni_{20}P_{20}$	569	644	75	881	0.65	3.41
$Pd_{40}Cu_{30}Ni_{10}P_{20}$ (*)	571	677	106	796	0.72	3.95
$Pd_{50}Cu_{20}Ni_{10}P_{20}$	597	690	93	917	0.65	6.43
$Pd_{60}Cu_{10}Ni_{10}P_{20}$	604	681	77	949	0.64	4.99
$Pd_{40}Ni_{25}Fe_{15}P_{20}$	603	676	73	955	0.64	6.25
$Pd_{40}Ni_{20}Fe_{20}P_{20}$	598	657	59	960	0.62	3.80

* Small ball with diameter about 2 mm.

Table 3

Room-temperature elastic constants, Young's modulus E, bulk modulus B, shear modulus G, Poisson's ratio ν, density ρ, and Debye temperature Θ_D for a number of Pd-Ni-P and Pd-Cu-P bulk amorphous alloys. The elastic moduli are in units of GPa and ρ is in units of g/cm^3.

Sample	C_{11}	C_{12}	C_{44}	E	B	G	ν	ρ	Θ_D (K)
$Pd_{25}Ni_{57}P_{18}$	232	152	40.0	112	179	40.0	0.396	8.97	311
$Pd_{40}Ni_{40}P_{20}$	229	156	36.6	103	180	36.6	0.405	9.36	286
$Pd_{50}Ni_{34}P_{16}$	230	152	39.2	110	178	39.2	0.397	9.84	285
$Pd_{40}Cu_{40}P_{20}$	202	136	33.2	93	158	33.2	0.402	9.30	269
$Pd_{50}Cu_{30}P_{20}$	205	139	32.7	92	161	32.7	0.405	9.46	262
$Pd_{60}Cu_{20}P_{20}$	210	145	32.3	91	167	32.3	0.409	9.78	254

REFERENCES

1. M. Schwarz, A. Karma, K. Eckler and D. M. Herlach, *Phys. Rev. Lett.*, 1994, vol. 73, pp. 1380-1383.
2. D. M. Herlach and R. Willnecker, in *Rapidly Solidified Alloys-Processes, Structures, Properties, Applications*, edited by H. H. Liebermann, Marcel Dekker, Inc., New York, NY, 1993, pp. 79-102.
3. J. H. Perepezko, *Mater. Sci. Eng.*, 1984, vol. 65, pp. 125-135; *ibid.*, 1994, vol. A178, pp. 105-111.
4. M. C. Flemings and Y. Shiohara, *Mater. Sci. Eng.*, 1984, vol. 65, pp. 157-170.
5. M. Barth, B. Wei, and D. M. Herlach, *Phys. Rev.* B, 1995, vol. 51, pp. 3422-3428.
6. D. Li, K. Eckler, and D. M. Herlach, *Acta Metall.*, 1996, vol. 44, pp. 2437-2443.
7. J. H. Perepezko and D. R. Allen, *Mater. Res. Soc. Symp.*, 1996, vol. 398, pp. 3-14.
8. D. Turnbull and R. E. Cech, *J. Appl. Phys.*, 1950, vol. 21, pp. 804-810.
9. D. Turnbull, *J. Chem. Phys.*, 1952, vol. 20, pp. 411-424.
10. D. M. Herlach, *Annu. Rev. Mater. Sci.*, 1991, vol. 21, pp. 23-44..
11. R. Willnecker, D. M. Herlach, and B. Feuerbacher, *Appl. Phys. Lett.*, 1986, vol. 49, pp. 1339-1341.
12. D. Holland-Moritz, D. M. Herlach, and K. Urban, *Phys. Rev. Lett.*, 1993, vol. 71, pp. 1196-1199.
13. D. M. Herlach, *Mater. Res. Soc. Symp. Proc.*, 1996, vol. 398, pp. 15-26.
14. G. Devaud and D. Turnbull, *Appl. Phys. Lett.*, 1985, vol. 46, 844-845.

15. M. Baricco, E. Ferrari, and L. Battezzati, *Mater. Res. Soc. Symp. Proc.*, 1996, vol. 398, pp. 81-86.

16. G. Wilde, G. P. Görler, and R. Willnecker, *Appl. Phys. Lett.*, 1996, vol. 68, pp. 2953-2955; *ibid.*, 1996, vol. 69, pp. 2995-2997.

17. Y. Shao and F. Spaepen, *J. Appl. Phys.*, 1996, vol. 79, pp. 2981-2985.

18. D. Turnbull and J. C. Fisher, *J. Chem. Phys.*, 1949, vol. 17, pp. 71-73.

19. D. Turnbull, *Contemp. Phys.*, 1969, vol. 10, pp. 473-488.

20. F. Spaepen and D. Turnbull, *Proceedings of 2nd International Conference on Rapidly Quenched Metals*, edited by N. J. Grant and B. C. Giessen (MIT Press, Cambridge, MA, 1976), pp. 205-227.

21. A. Inoue, A. Kato, T. Zhang, S. G. Kim, and T. Masumoto, *Mater. Trans. JIM*, 1991, vol. 32, pp. 609-616.

22. A. Inoue, T. Nakamura, N. Nishiyama, and T. Masumoto, *Mater. Trans. JIM*, 1992, vol. 33, pp. 937-945.

23. A. Inoue, T. Nakamura, T. Sugita, T. Zhang, and T. Masumoto, *Mater. Trans. JIM*, 1993, vol. 34, pp. 351-358.

24. A. Peker and W. L. Johnson, *Appl. Phys. Lett.*, 1993, vol. 63, pp. 2342-2344.

25. Y. He, C. E. Price, S. J. Poon, and G. J. Shiflet, *Phil. Mag. Lett.*, 1994, vol. 70, pp. 371-377.

26. A. Inoue and T. Zhang, *Mater. Trans. JIM*, 1996, vol. 37, pp. 185-187.

27. X. H. Lin and W. L. Johnson, *J. Appl. Phys.*, 1995, vol. 78, pp. 6514-6519.

28. H. S. Chen, *Acta Metall.*, 1974, vol. 22, pp. 1505-1511.

29. A. J. Drehman, A. L. Greer, and D. Turnbull, *Appl. Phys. Lett.*, 1982, vol. 41, pp. 716-717.

30. H. W. Kui, A. L. Greer, and D. Turnbull, *Appl. Phys. Lett.*, 1984, vol. 45, pp. 615-616.

31. Y. He, R. B. Schwarz, and J. I. Archuleta, *Appl. Phys. Lett.*, 1996, vol. 69, pp. 1861-1863.

32. R. B. Schwarz and Y. He, *International Symposium on Metastable. Mechanically Alloyed and Nanocrystalline Materials* (*ISMNAN-96*), Rome, Italy, 20-24 May, 1996, in press.

33. Y. He and R. B. Schwarz, *Mater. Res. Soc. Symp. Proc.*, vol. 455, "Structure and Dynamics of Glass and Glass Formers", edited by C. A. Angell, T. Egami, J. Kieffer, U. Nienhaus, and K. L. Ngai, to be published.

34. M. J. O'Neil, *Anal. Chem.*, 1966, vol. 38, pp. 1331-1336.

35. A. L. Greer, *Nature*, 1993, vol. 366, pp. 303-304.

36. R. B. Schwarz and Y. He, *Proceedings of the First International Alloy Conference* (*IAC-1*), June 16-21, 1996, Athens, Greece.

37. H. S. Chen, *Acta Metall.*, 1974, vol. 22, pp. 897-900.

38. H. S. Chen, *Mater. Sci. Eng.*, 1976, vol. 23, pp. 151-154.

39. F. R. de Boer, R. Boom, W. C. M. Mattens, A. R. Miedema. and A. K. Niessen, *Cohesion in Metals*, 1988, North Holland, Amsterdam.

40. M. H. Cohen and D. Turnbull, *J. Chem. Phys.*, 1959, vol. 31, pp. 1164-1169.

41. D. Turnbull and M. H. Cohen, *J. Chem. Phys.*, 1961, vol. 34, pp. 120-125.

42. D. Turnbull and M. H. Cohen, *J. Chem. Phys.*, 1970, vol. 52, pp. 3038-3041.

43. M. H. Cohen and G. S. Grest, *Phys. Rev. B*, 1979, vol. 20, pp. 1077-1098.

44. A. van den Beukel and J. Sietsma, *Acta Metall. Mater.*, 1990, vol. 38, pp. 383-389.

45. H. S. Chen, *Mater. Sci. Eng.*, 1976, vol. 23, pp. 151-154.

46. J. Jing, U. Gonser, and H. G. Wagner, *Z. Metallkunde*, 1987, vol. 78, pp. 767-769.

47. T. Egami, W. Dmowski, Y. He, and R. B. Schwarz, this volume.

48. "Binary Alloy Phase Diagrams", edited by T. B. Massalski, H. Okamoto, P. R. Subramanian, and L. Kacprzak (ASM, Metals Park, 1996).

49. P. E. Donovan, P. V. Evans and A. L. Greer, *J. Mater. Sci. Lett.*, 1986, vol. 5, pp. 951-952.

50. C. F. Lau and H. W. Kui, *J. Appl. Phys.*, 1993, vol. 73, pp. 2599-2601.

51. A. J. Drehman and A. L. Greer, *Acta Metall.*, 1984, vol. 32, pp. 323-332.

52. R. Willnecker, K. Wittmann, and G. P. Görler, *J. Non-Cryst. Solids*, 1993, vol. 156-158, pp. 450-454.

53. Y. He and R. B. Schwarz, unpublished results, Los Alamos National Laboratory, 1996.

54. G. Wilde, G. P. Görler, R. Willnecker and G. Dietz, *Appl. Phys. Lett.*, 1994, vol. 65, pp. 397-399.

55. Y. J. Kim, R. Busch, W. L. Johnson, A. J. Rulison, and W. K. Rhim, *Appl. Phys. Lett.*, 1994, vol. 65, pp. 2136-2138.

56. A. Migliori, J. L. Sarrao, W. M. Visscher, T. M. Bell, M. Lei, Z. Fisk, and R. G. Leisure, *Physica* B, 1993, vol. 183, pp. 1-24.

57. V. -T. Kuokkala and R. B. Schwarz, *Rev. Sci. Instrum.*, 1992, vol. 63, pp. 3136-3142.

58. J. D. Maynard, *J. Acoust. Soc. Am.*, 1992, vol. 91, pp. 1754-1762.

59. D. R. Nelson and F. Spaepen, in *Solid State Physics*, 1989, vol. 42, pp. 1-90, eds. H. Ehrenreich and D. Turnbull, Academic Press, New York.

60. P. L. Maitrepierre, *J. Appl. Phys.*, 1969, vol. 40, pp. 4826-4834.

61. A. Inoue, T. Zhang, and T. Masumoto, *Mater. Trans. JIM*, 1990, vol. 31, pp. 425-428.

62. D. Turnbull, *Metall. Trans.*, 1981, vol. 12A, pp. 695-708.

63. J. B. Rubin and R. B. Schwarz, *Phys. Rev. B*, 1994, vol. 50, pp. 795-804.

64. T. Egami and Y. Waseda, *J. Non-Cryst. Solids*, 1984, vol. 64, pp. 113-134..

65. H. G. Jiang and J. Baram, *Mater. Sci. Eng.*, 1996, vol. A208, pp. 232-238.

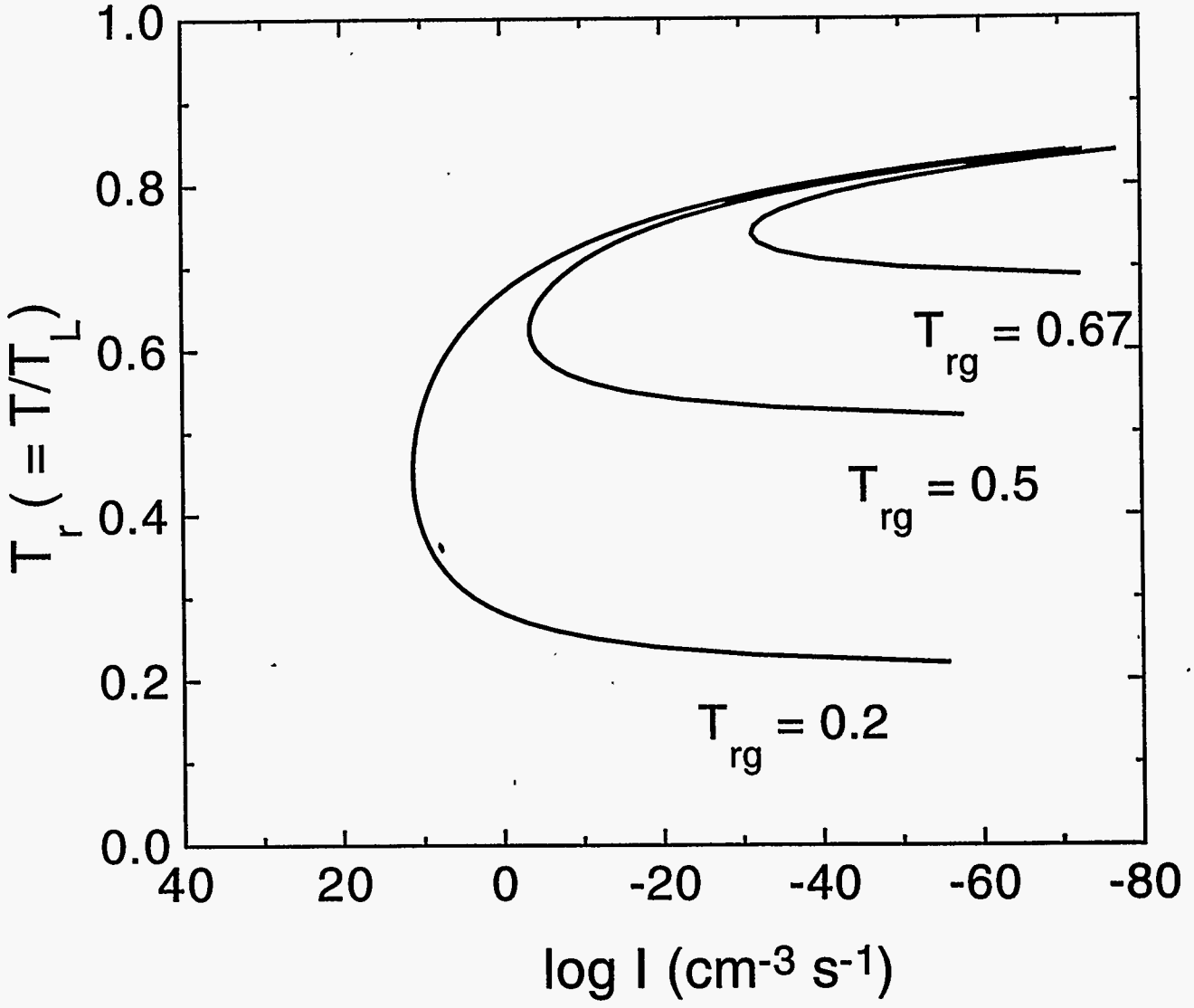

He, Shen, Schwarz, Fig 1

e:\Papers\TMS1997\Nucleate.org-Plot2

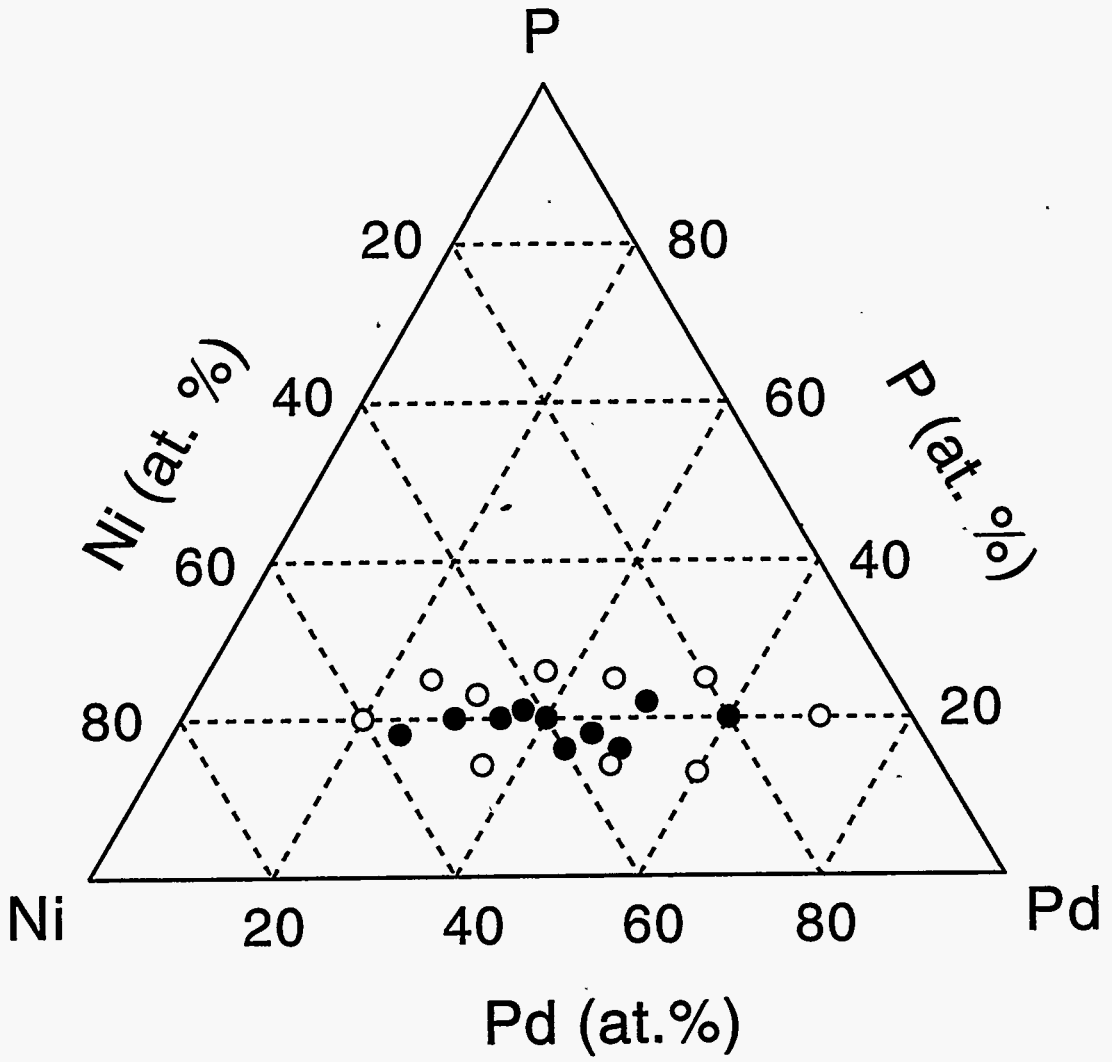

Fig. 2

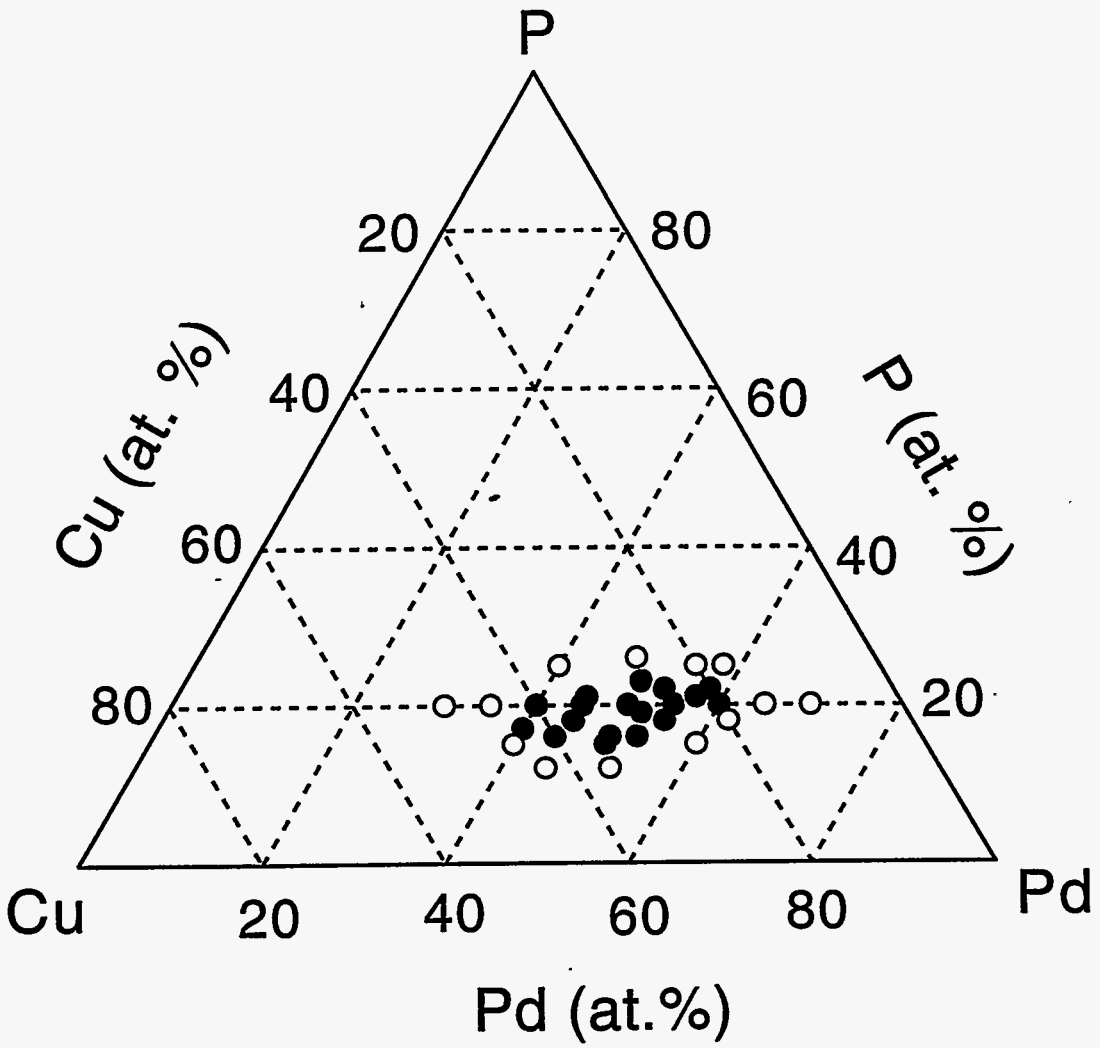

Fig. 3

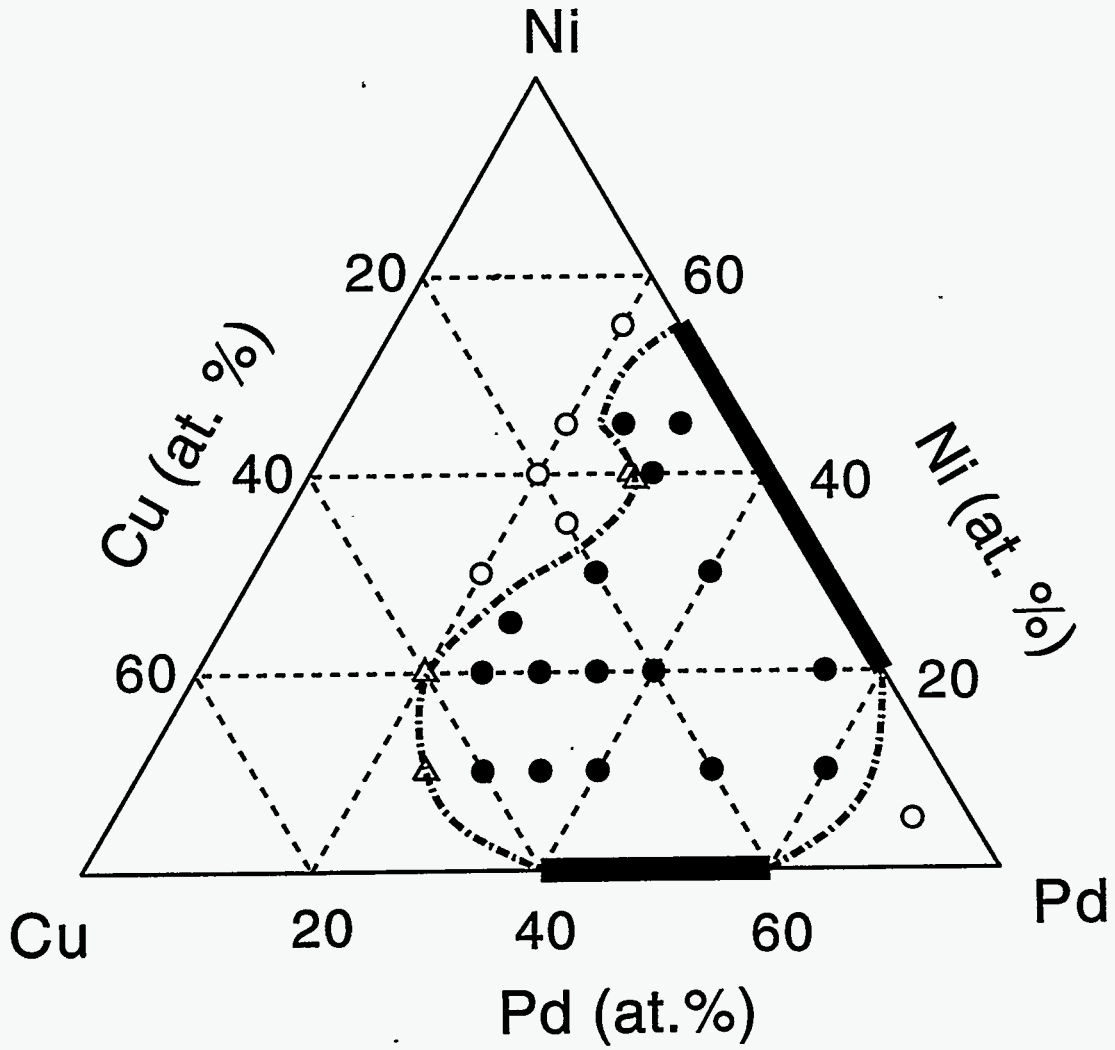

Fig. 4

d:\PdCuNiP.org

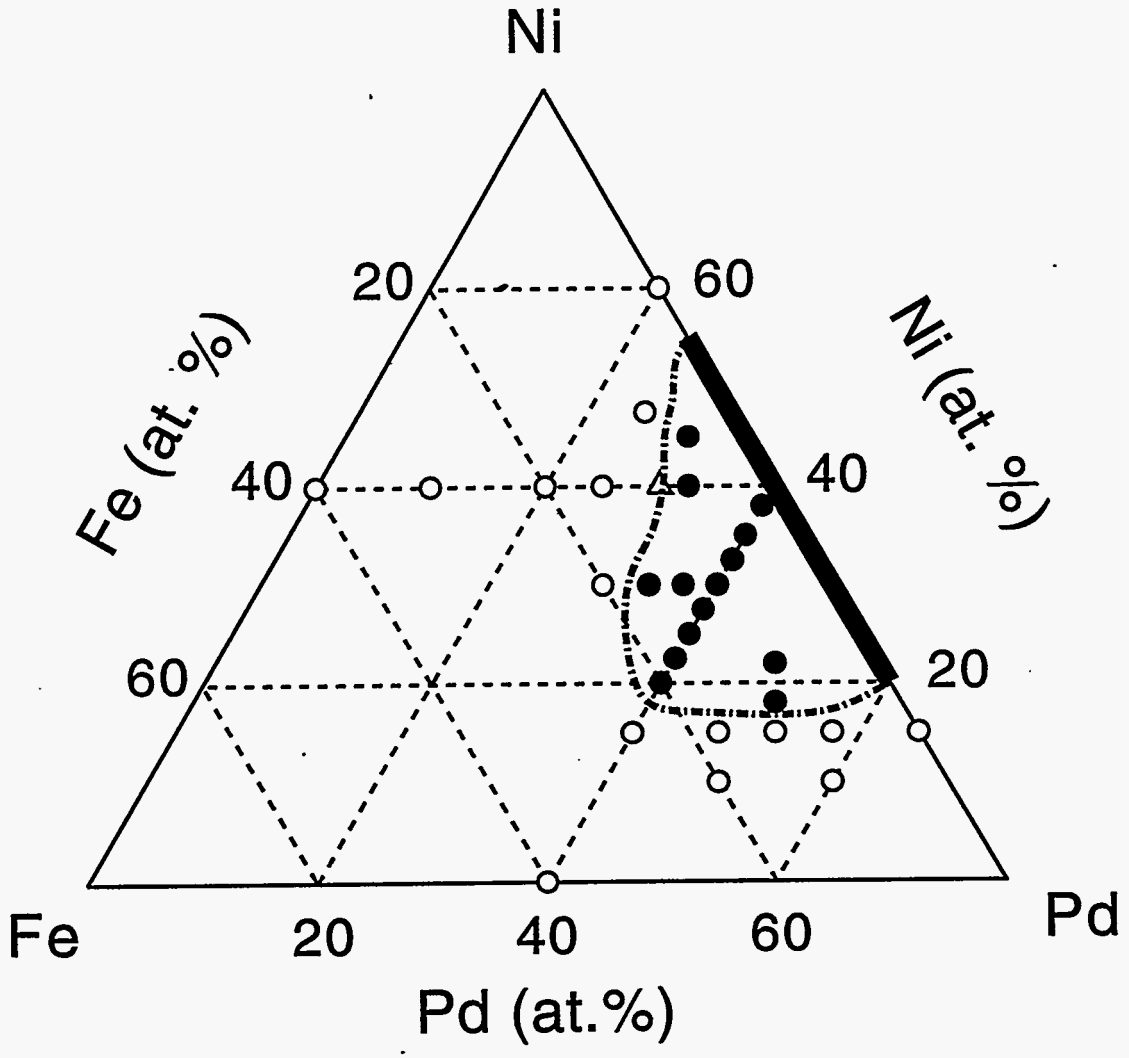

Fig. 5

dAPdFeNiP.opj

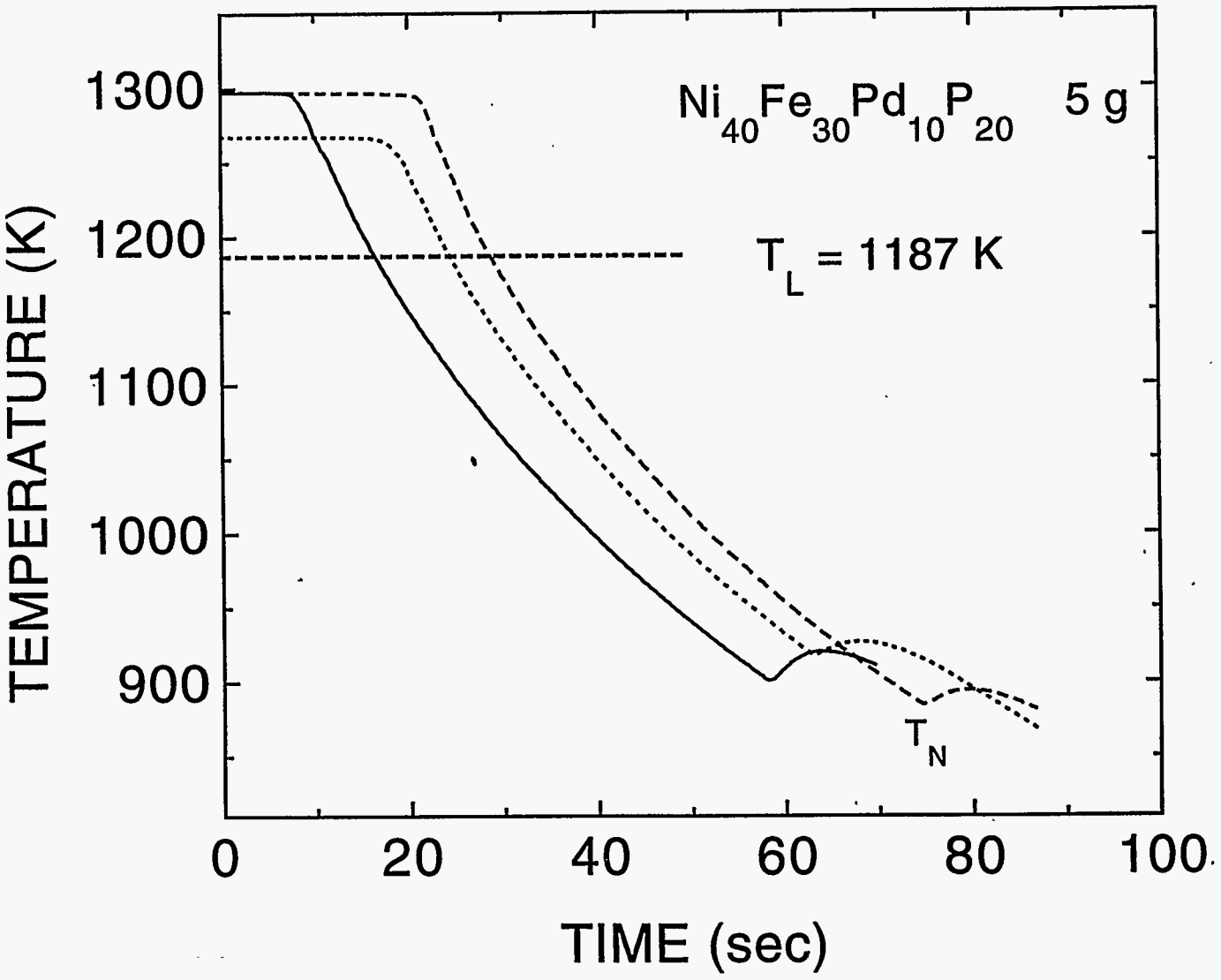
1300
1200
1100
1000
900
TEMPERATURE (K)
0
20
40
60
80
100
TIME (sec)
Ni40Fe30Pd10P20 5 g
TL = 1187 K
TN

Fig. 6

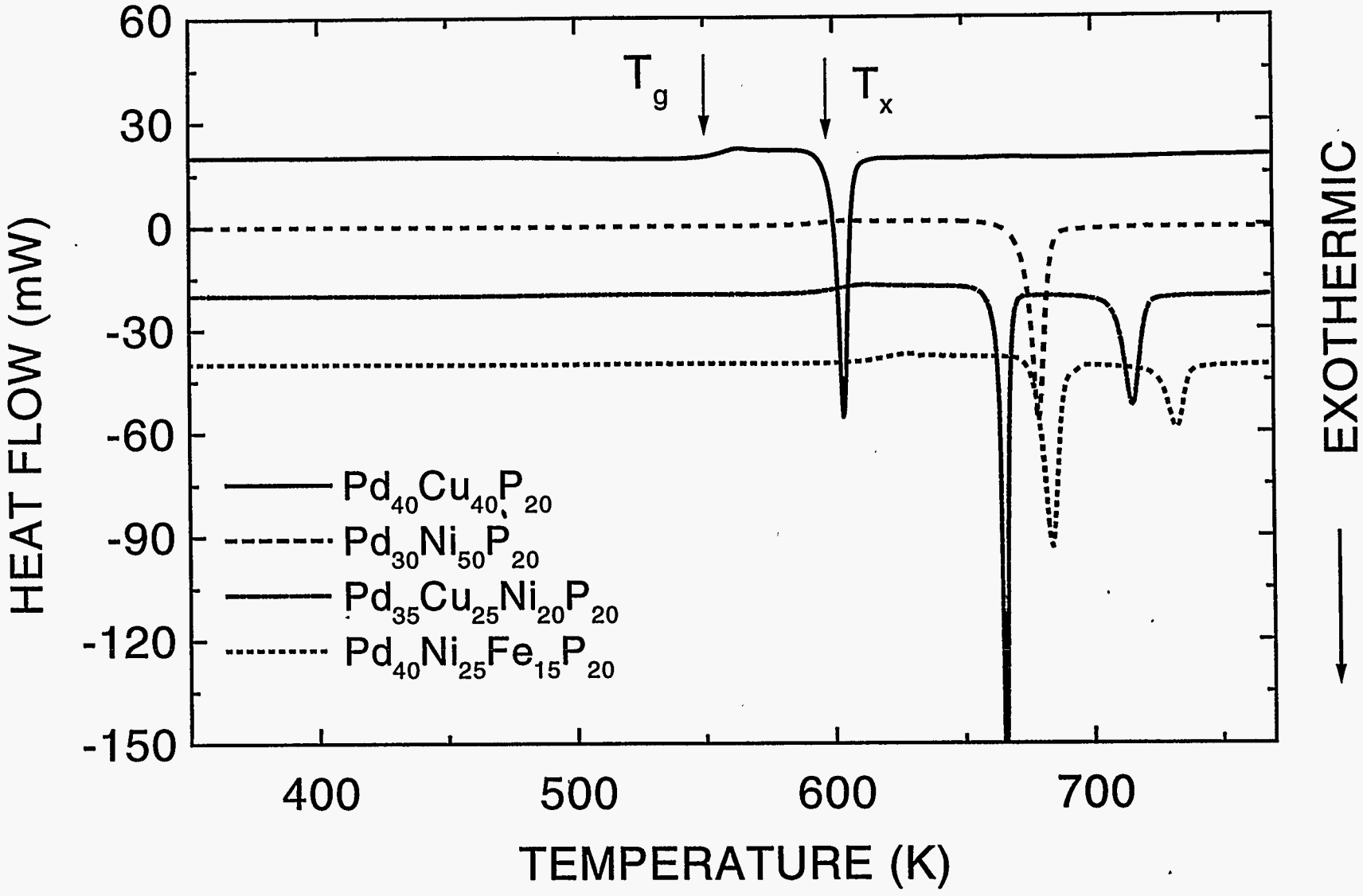

e\Papers\TMS1997\DSC.org

Fig. 7

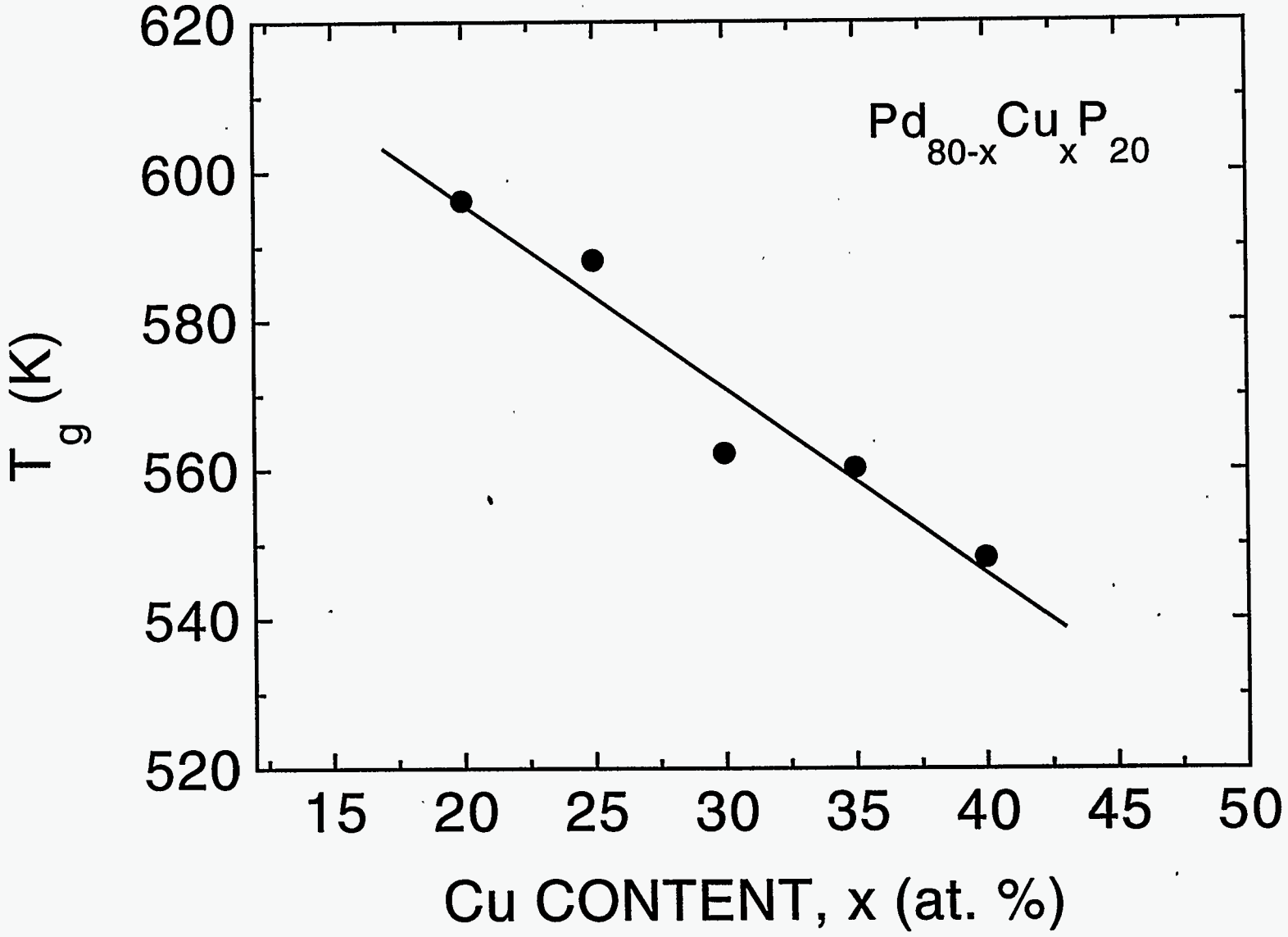

Fig. 8

e:\Papers\TMS1997\Tg.org-graph1

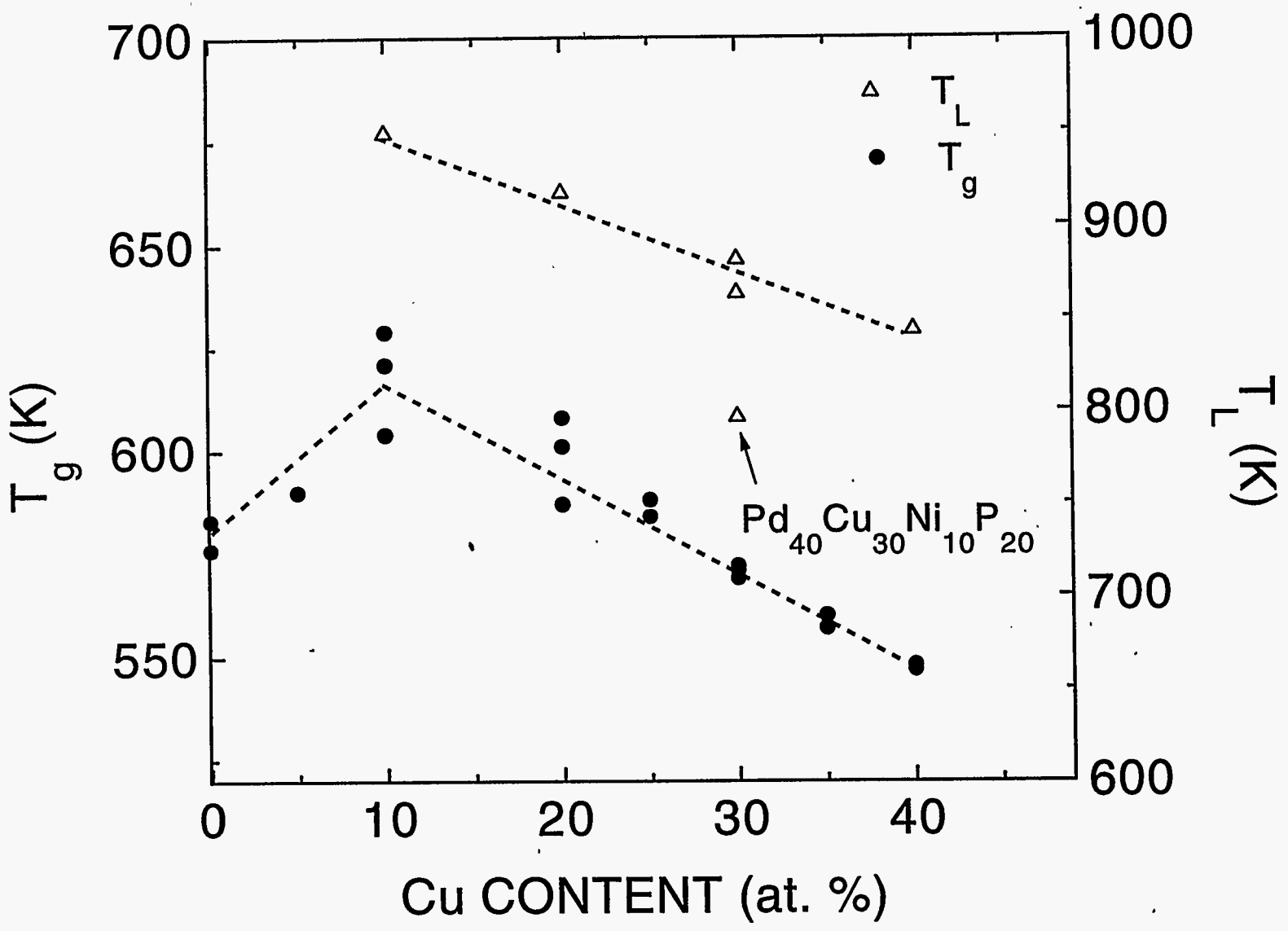
700
650
600
550
1000
900
800
700
600
T_g (K)
T_L (K)
T_L
T_g
$Pd_{40}Cu_{30}Ni_{10}P_{20}$
0
10
20
30
40
Cu CONTENT (at. %)
e:\Papers\TMS1997\Tg.org--Plot7

Fig. 9

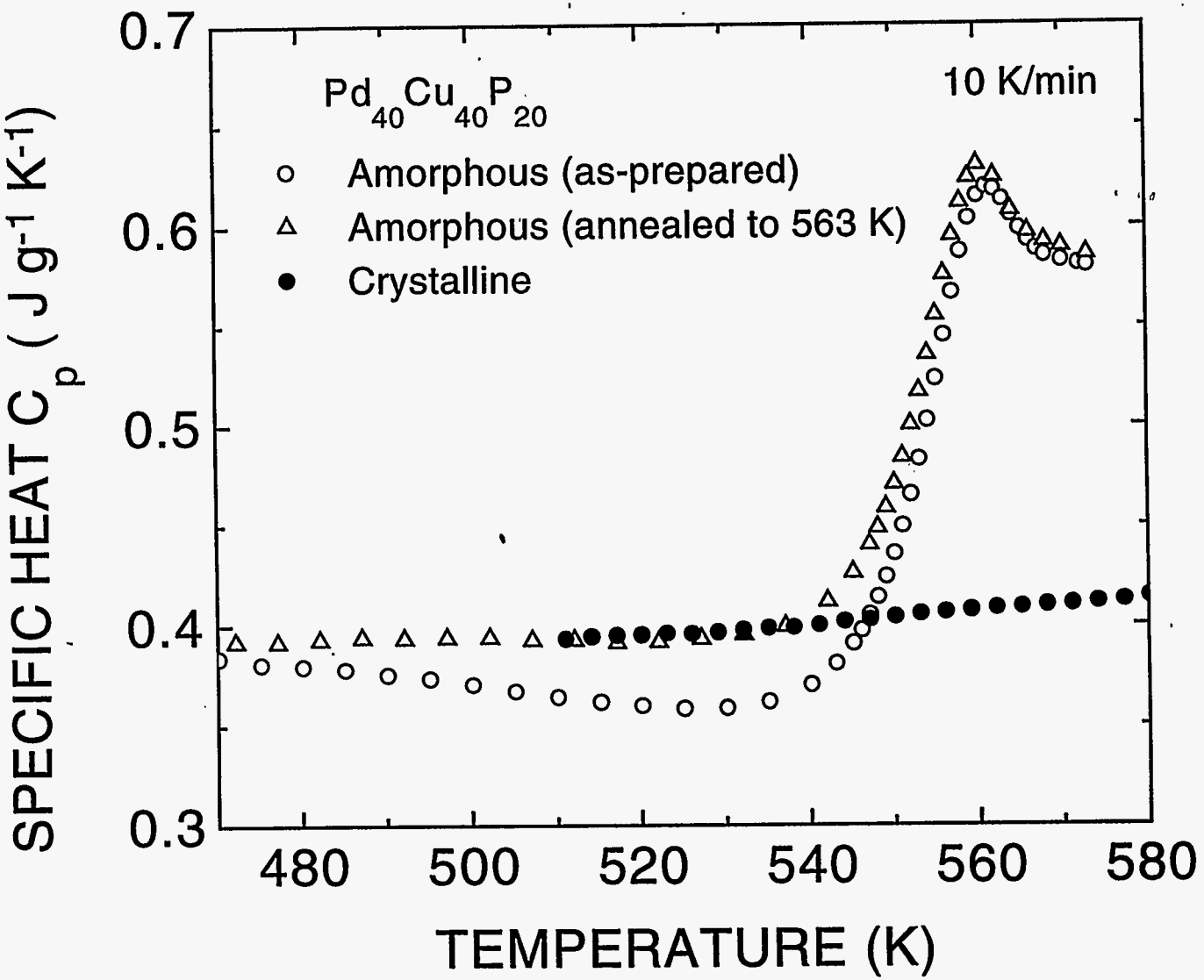

Fig. 10

e:\Papers\PdCuPCp.org-Plot1

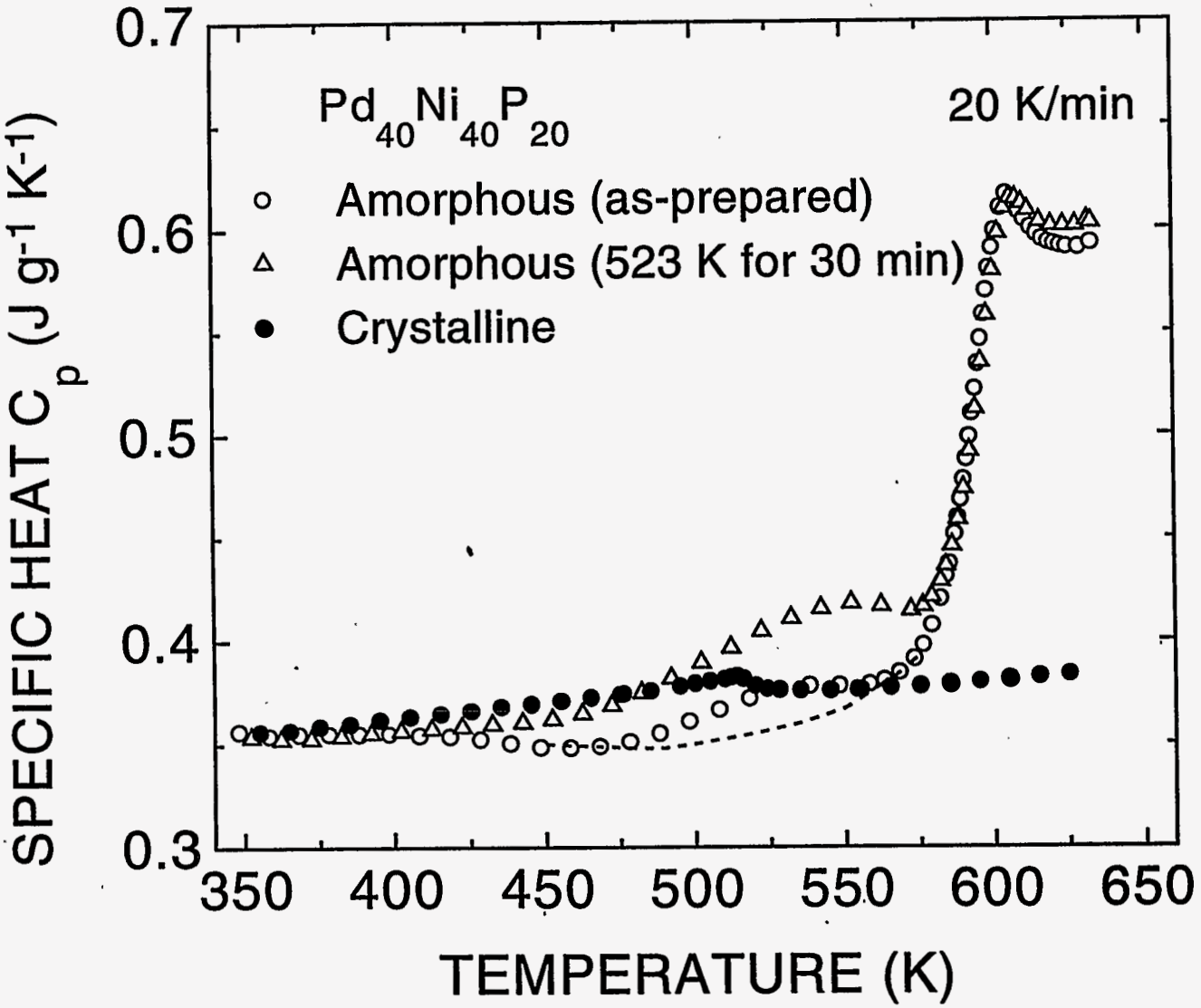

Fig. 11

e:\Papers\TMS1997\PdNiPCp.org--Plot3

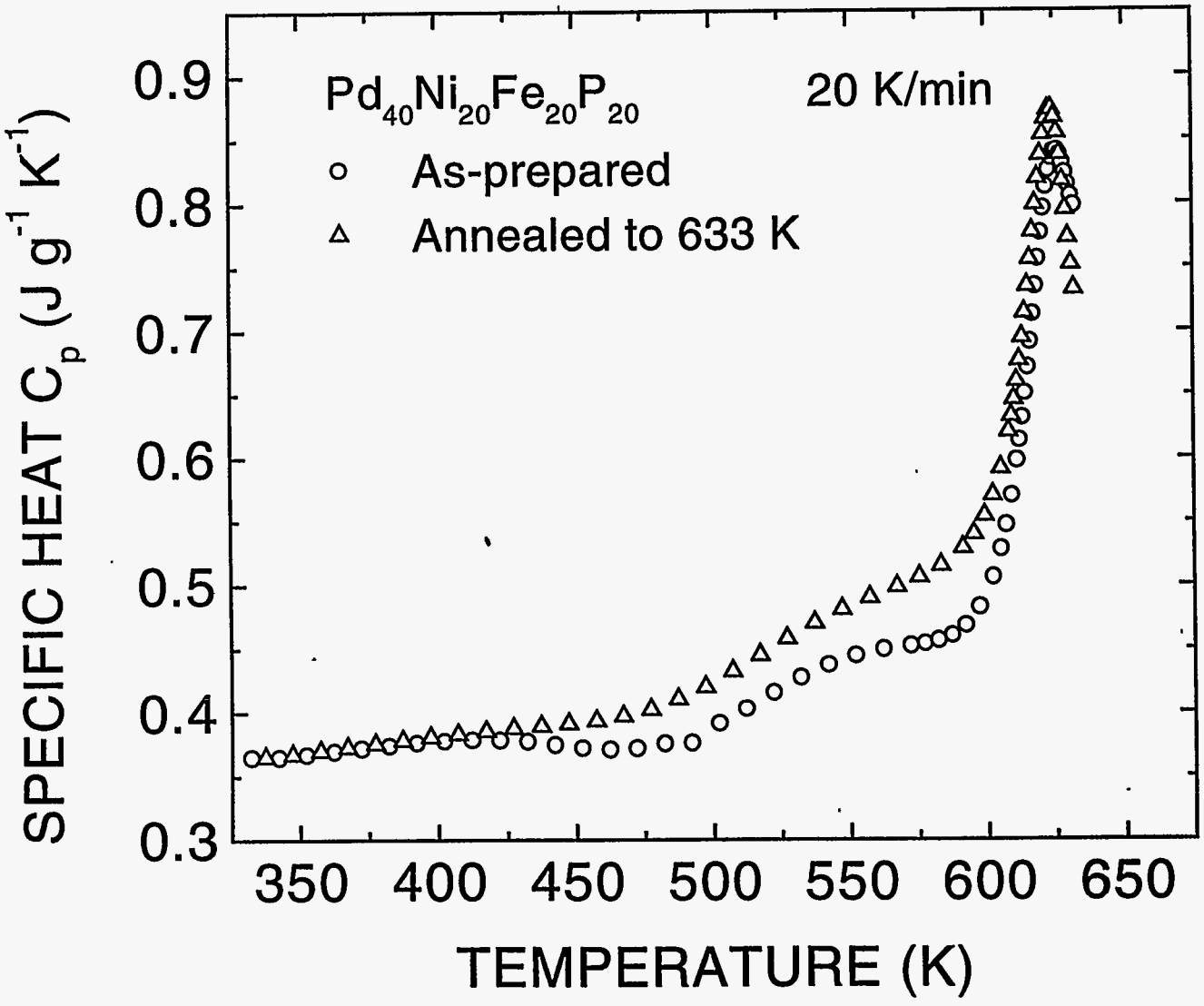

Fig 12

e:\Papers\TMS1997\NiFe20Cp.opj-Graph4

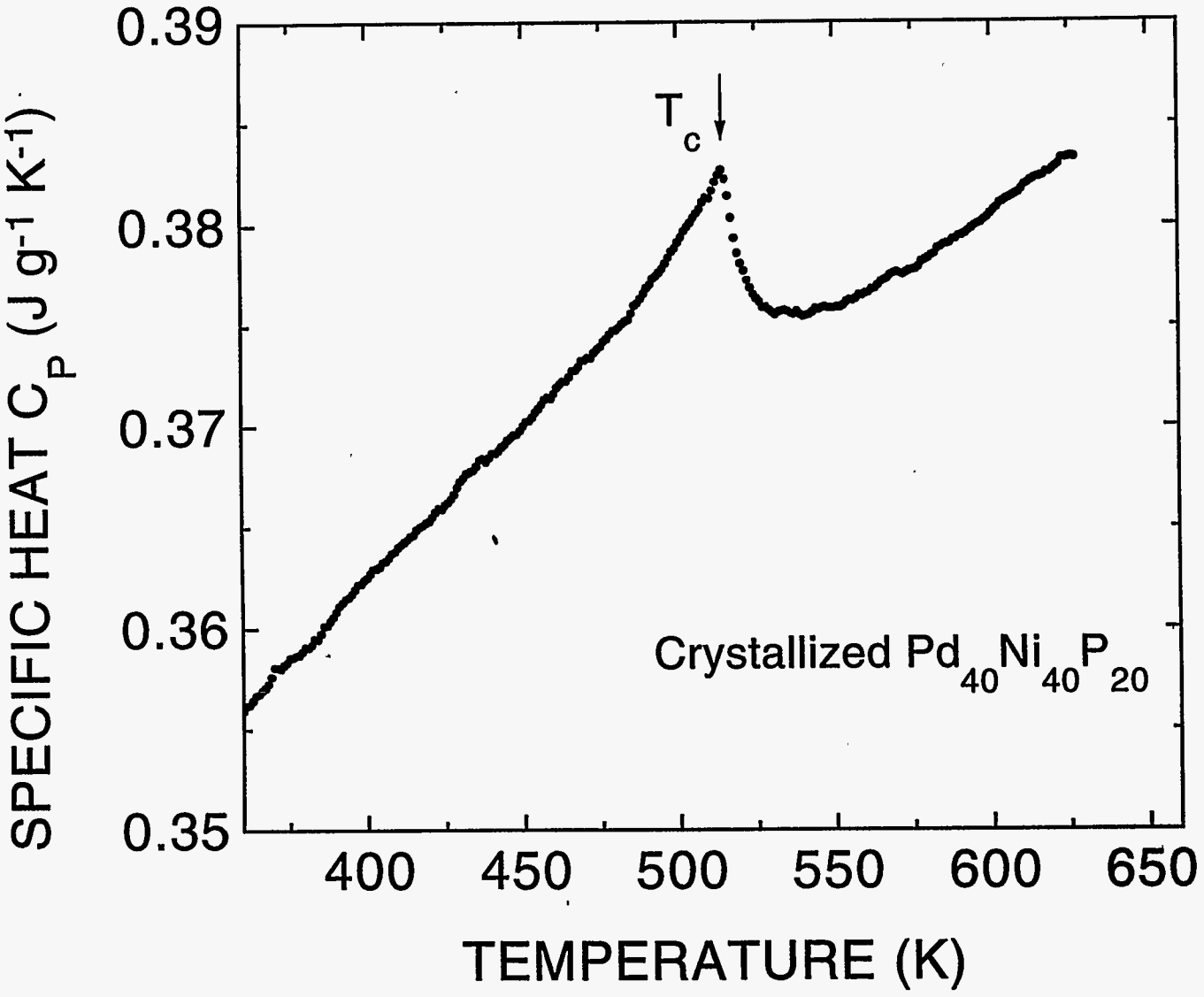

Fig. 13

e:\Papers\TMS1997\PdNiPCp.org-Plot2

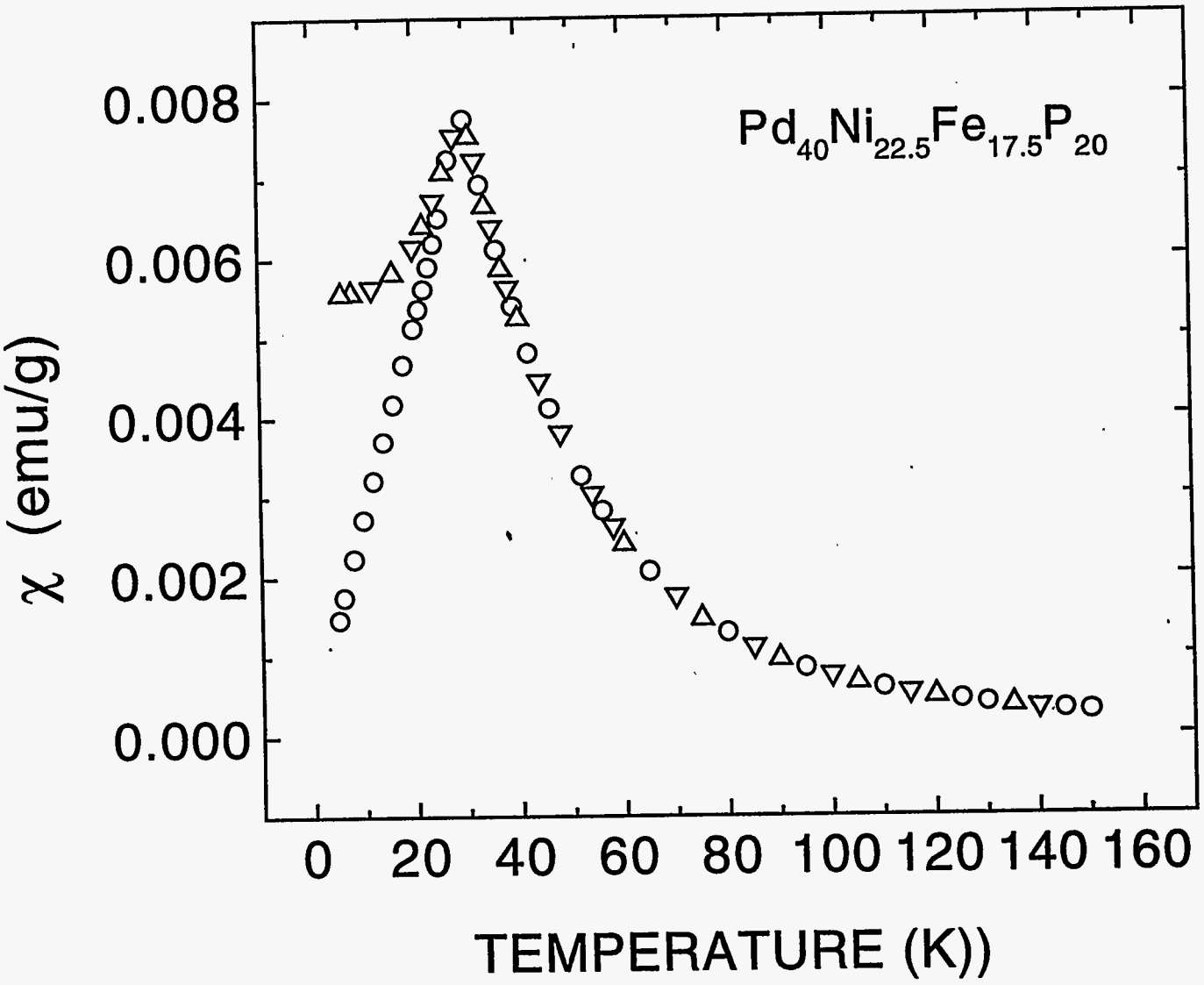

Fig. 14

e:\Papers\TMS1997\Fe17xtg.opj-Graph6